(Received 26 October 2023, Accepted 30 November 2023, Scheduled 12 December 2023)

Solving Electromagnetic Wave Scattering Using Artificial Neural Networks

Mohammad Ahmad*

Department of Electrical and Mechanical Engineering, Applied Science University, Eker, Kingdom of Bahrain

ABSTRACT: Electromagnetic wave scattering (EMWS) is one of the complexities in electromagnetism. Traditionally, three numerical methods are used to solve this problem which are finite element method, finite difference method, and method of moments. Recently, artificial neural networks (ANNs) have gained popularity as tools to solve different problems in a wide variety of disciplines, including electromagnetism. This paper shows that the second order differential equation that represents EMWS from one-dimensional, two-dimensional, and three-dimensional homogeneous mediums and deals with complex numbers can be solved using ANN. This is done by reducing the error between the trail solution at the output of the ANN and the second ordinary differential equation that represents the scattered field. The results from solving classical examples using the suggested approach are accurate.

1. INTRODUCTION

Electromagnetic wave scattering problem (EMWS) is one important class of electromagnetic boundary value problems (EMBVPs) [1]. Traditionally, it has been solved using the finite element method (FEM) [2, 3] and finite difference method [4, 5] if Maxwell's equations are formulated in terms of partial differential equations or method of moments [6, 7] if they are formulated in terms of integral equations. Solving the EMWS using these methods requires a discrete grid system which will produce matrix equations that are solved using inversions or iterative methods [8].

Originally, artificial neural networks (ANNs) were used to solve simple problems such as regression, classification, and clustering [9]. However, the fast growth in computer and data sciences has inspired researchers to test the potential of using ANNs in more varied and complex applications such as image classification [10] and segmentation [11], language processing [12], human-centered robotics [13], and optical imaging system [14–16]. Recently, a limited number of researchers have started using ANNs to solve some problems in electromagnetics [17–19], antenna design [20], radar, and remote sensing [21, 22].

For EMBVPs, [23] suggests a solution for both partial differential equations and ordinary differential equations using ANNs. However, their method is limited to homogeneous medium, dealing with real numbers and uniform boundaries. While [24] suggests a method based on ANNs that deals with the case of irregular boundaries, [25] deals with mixed Dirichlet and/or Neumann boundary conditions (BCs) with irregular boundaries. However, both methods are limited to homogeneous mediums and deal with real numbers. In [26], the authors solved Poisson's equation and Helmholtz's equation. However, the proposed method deals with homogeneous mediums. In [27], the authors dealt with inhomogeneous mediums and complex numbers by solving second order differential equations (2-ODE) with analytical solution first for several values of given ε_r where ε_r is the relative permittivity of a medium and then using ANNs to predict the solution based on the analytical solution of other values of ε_r. Different from [27], the proposed approach in this paper does not predict the solution based on previously solved samples and then feeds them to the ANNs. It solves the 2-ODE by reducing the error between the trail solution at the output of the ANNs and the 2-ODE that represents the scattered field.

The contribution of this paper can be summarized as the first work dedicated solely to solving the 2-ODE that represents EMWS from one-dimensional (1D), two-dimensional (2D), and three-dimensional (3D) homogeneous mediums and deals with complex numbers using ANN.

The framework of this manuscript is as follows. The general 2-ODE that represents the 3D EMWS is presented, with 1D and 2D problems being special cases of the 3D problem. Next, the solution of the 2-ODE using ANNs is discussed in detail. Finally, EMWS from 1D, 2D, and 3D perfect electric conductors (PECs) and dielectric objects are solved using the proposed approach and FEM for the sake of comparison.

2. FORMULATION OF THE PROBLEM

2.1. General Second Order Differential Equation

Consider a 3D PEC or dielectric object of arbitrary cross-section, illuminated by a plane wave centered at the origin as shown in Fig. 1. For an isotropic and non-magnetic medium ($\mu_r = 1$ where μ_r is relative permeability) and TM_e where e represents the electric field direction of polarization (x, y or z),

* Corresponding author: Mohammad Ahmad (mohd.ahmad@asu.edu.bh).

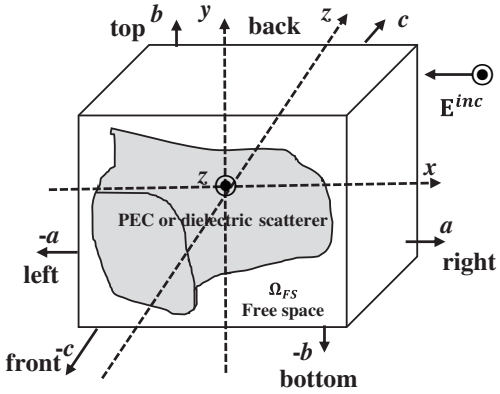

FIGURE 1. 3D electromagnetic scattering problem.

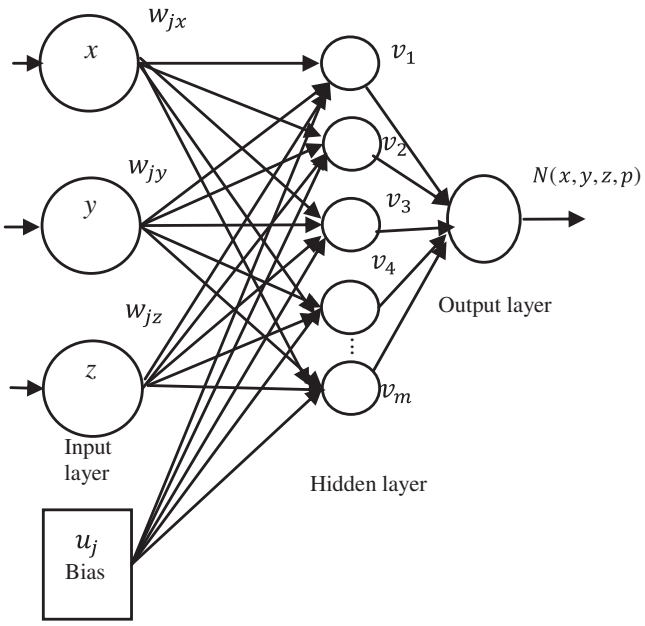

FIGURE 2. Structure of multilayer ANN.

the scattered field satisfies the following 2-ODE [3]

$$-\frac{\partial^2 E_e^{scat}}{\partial x^2}-\frac{\partial^2 E_e^{scat}}{\partial y^2}-\frac{\partial^2 E_e^{scat}}{\partial z^2}-k_0^2\varepsilon_{rc}E_e^{scat}$$

$$=\ k_0^2\left(\varepsilon_{rc}-1\right)E_e^{inc} \tag{1}$$

where $(x, y, z) \in \Omega$, E_e^{scat} is the unknown scattered field to be determined; $k_0 = \omega\sqrt{\varepsilon_0\mu_0}$ is the free-space wavenumber with $\omega = 2\pi f$; f is the frequency; $\varepsilon_0 = 8.85\times10^{-12}$ F/m; $\mu_0 = 4\pi \times 10^{-7}$ H/m; $\varepsilon_{rc} = \varepsilon_r - j\sigma/\omega\varepsilon_0$ is the complex relative permittivity; σ is the conductivity; E_e^{inc} is the incident field.

2.2. Structure of the ANNs

The following solution is proposed by [23] to solve ordinary and partial differential equations with real numbers only and homogenise mediums. Since most EMWS problems deal with complex numbers, their method is modified to accommodate them with the help of [28]. The design of an ANN contains a three-input node x, y, and z along with biases u_j, a hidden layer containing m neurons, and one output node at the output layer. The weights from the input layer to the hidden layer are w_{jx}, w_{jy}, and w_{jz} and from the hidden layer to the output layer are v_j where $j = 1, 2, \ldots, m$ as shown in Fig. 2.

The output from the output layer is

$$N\left(x,y,z,p\right)=\sum_{j=1}^{m}v_j f_C(Y_j) \tag{2}$$

where p are the adjustable parameters (weights and biases), $Y_j = w_{jx}x+w_{jy}y+w_{jz}z+u_j$, and $f_C(Y_j)$ is the activation function. Note that w_{jx}, w_{jy}, w_{jz}, v_j, and u_j are complex numbers.

2.3. Solution of 2-ODE Using ANNs

The trial solution of (1) is

$$y_t\left(x,y,z,p\right)=A\left(x,y,z\right)+F(x,y,zN(x,y,z,p)) \tag{3}$$

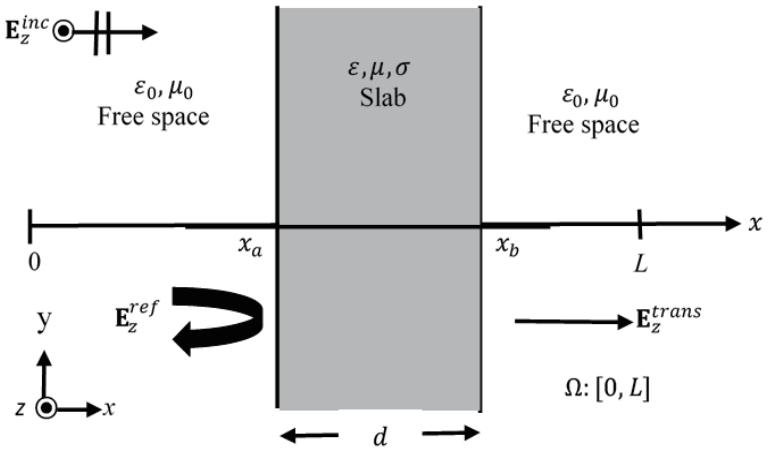

FIGURE 3. Geometry of 1D EM scattering from a lossy dielectric slab.

where $A(x,y,z)$ satisfies the BCs. The term $F(x,y,z,N(x,y,z,p))$ is the output of the ANN whose biases and weights are updated to reduce the error function to get the best ANN solution. The error function for 2-ODE is:

$$E(x,y,z,p) = \sum_{c_z=1}^{h_z}\sum_{c_y=1}^{h_y}\sum_{c_x=1}^{h_x} \frac{1}{2}\left(\left(-\frac{\partial^2 y_t\left(x_{c_x},y_{c_y},z_{c_z},p\right)}{\partial x^2}-\frac{\partial^2 y_t\left(x_{c_x},y_{c_y},z_{c_z},p\right)}{\partial y^2} -\frac{\partial^2 y_t\left(x_{c_x},y_{c_y},z_{c_z},p\right)}{\partial z^2}-k_0^2\varepsilon_{rc}y_t\left(x_{c_x},y_{c_y},z_{c_z},p\right)\right) -k_0^2(\varepsilon_{rc}-1)E_e^{inc}\right)^2 \quad (4)$$

where h_x, h_y, and h_z are the amount of data for x, y, and z, respectively.

The weights and biases should be modified according to the following equations:

$$w_{jh}^{n+1} = w_{jh}^n - \eta\left(\frac{\partial E(x,y,z,p)^n}{\partial Re[w_{jh}^n]} + i\frac{\partial E(x,y,z,p)^n}{\partial Im[w_{jh}^n]}\right) \quad (5a)$$

$$v_j^{n+1} = v_j^n - \eta\left(\frac{\partial E(x,y,z,p)^n}{\partial Re[v_j^n]} + i\frac{\partial E(x,y,z,p)^n}{\partial Im[v_j^n]}\right) \quad (5b)$$

$$u_j^{n+1} = u_j^n - \eta\left(\frac{\partial E(x,y,z,p)^n}{\partial Re[u_j^n]} + i\frac{\partial E(x,y,z,p)^n}{\partial Im[u_j^n]}\right) \quad (5c)$$

where h represents x, y, and z, respectively in three versions; Re represents a real part; Im represents an imaginary part; η is the learning parameter; and n is the iteration step.

3. RESULTS AND DISCUSSION

All numerical examples were solved on a Laptop with an Intel Core i5-4300U CPU equipped with 8 GB RAM. The mean percentage error (MSE) is

$$MSE = \frac{\sum_{n=1}^{N}\left[V_n^{proposed\ method\ solution} - V_n^{reference\ solution}\right]^2}{\left[V_n^{reference\ solution}\right]^2}$$

where $V_n^{reference\ solution}$ in all examples is the solution for the same problem using FEM. Also, the activation function that has been used in all examples is the sigmoid which is given by $f_c(Y) = 1/(1+e^{-Y})$. In addition, the number of nodes in the hidden layer is assumed to be $m = 5$. Finally, the learning parameter $\eta = 0.1$ is selected for all examples.

3.1. One Dimensional EMWS

The problem to be considered is shown in Fig. 3. A uniform plane wave is propagating along the $+x$ direction and incident upon an homogeneous and lossy dielectric slab occupying the region $x_a \le x \le x_b$. When the plane wave is incident onto the slab, some will reflect $\mathbf{E}_z^{ref}$, and the rest wave will transmit through the slab $\mathbf{E}_z^{trans}$.

The total field, i.e., E_z^{total}, is defined as [3]

$$E_z^{total} = E_z^{scat} + E_z^{inc}.$$

Equation (1) becomes

$$-\frac{\partial^2 E_z^{scat}}{\partial x^2} - k_0^2\varepsilon_{rc}E_z^{scat} = k_0^2(\varepsilon_{rc}-1)E_z^{inc} \quad (6)$$

where $E_z^{inc} = \exp(-jk_0x)$, and $\hat{a}_z$ is the unit vector along the direction of incidence.

The problem is unbounded. Hence, a uniaxial perfectly matched layer (UPML) is used to absorb the outgoing fields. Incorporating UPML in the solution is described in detail for 3D general case in [1, pp. 96-102].

The solution of (6) using the proposed method for this example is done as follows:

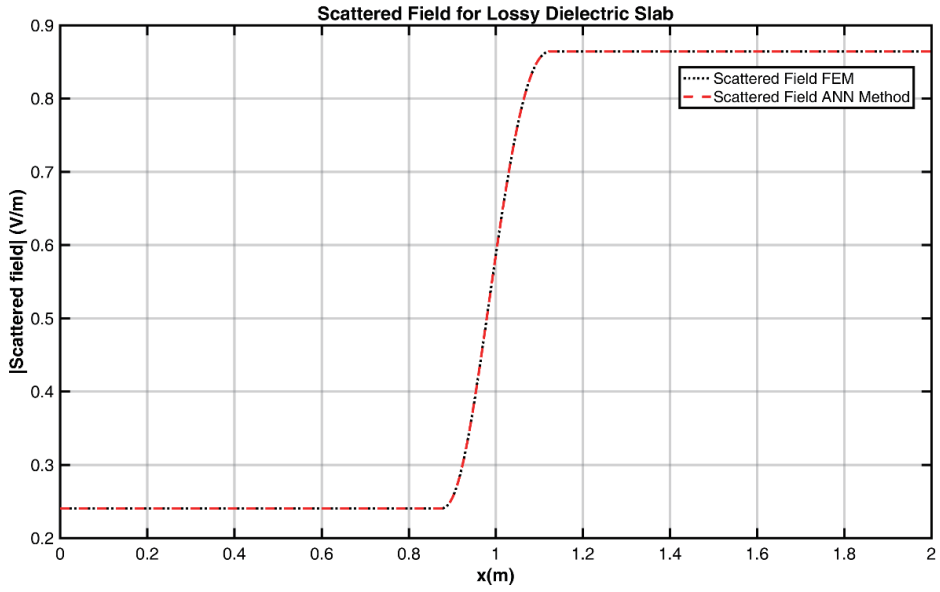

FIGURE 4. Absolute value for the scattered field solved by ANN method and FEM.

1. Initialize values for w_{jx}, v_j, and u_j using MATLAB function "rand" where $j = 1, 2, \ldots, 5$. The ANN was trained using a grid of h_x =1000 equidistant points in $x \in [0, L]$, i.e., $c_x = 1, 2, 3, \ldots, h_x$ in (4).

2. Determine the trial solution using (3)

$$y_t(x,p) = E^{scat}_{ztrial} = N(x,p)$$

where $N(x,p) = \frac{v_1}{1+e^{-(w_{1x}x+u_1)}} + \frac{v_2}{1+e^{-(w_{2x}x+u_2)}} + \frac{v_3}{1+e^{-(w_{3x}x+u_3)}} + \frac{v_4}{1+e^{-(w_{4x}x+u_4)}} + \frac{v_5}{1+e^{-(w_{5x}x+u_5)}}$ and $A(x) = 0$.

3. Use (4) to find the error, i.e.,

$$E(x,p) = \sum_{c_x=1}^{h_x=1000} \frac{1}{2}\left(\left(-\frac{\partial^2 y_t(x_{c_x},p)}{\partial x^2} - k_0^2 \varepsilon_{rc} y_t(x_{c_x},p)\right) - k_0^2(\varepsilon_{rc}-1)E_z^{inc}\right)^2.$$

4. Check the error, if the error $\leq$ the required error, stop. Otherwise, use (5) to adjust the old values of w_{jx}, v_j, and u_j.

5. Repeat step 3 until you get the required error.

The following parameters are used, the frequency is 300 MHz, $L = 2$ m, $d = \lambda/4$, $\varepsilon_r = 2.7$, and $\sigma = 5 \times 10^{-3}$ S/m. The scattered field has been found using the proposed method. MSE = 7.69×10^{-3} for all points of solution. Fig. 4 shows the absolute value for the scattered field solved using ANN method and FEM.

3.2. Two Dimensional EMWS

The problem to be considered is EMWS from PEC or a dielectric circular cylinder. Since the domain of interest extends to infinity, UPML is used. The incident field for this example is assumed to be $E_z^{inc} = \exp(jk_0 x)\hat{a}_z$. Also, $f = 3 \times 10^8/\lambda$ Hz and $\lambda = 1$ m are assumed.

Equation (1) becomes

$$-\frac{\partial^2 E_z^{scat}}{\partial x^2} - \frac{\partial^2 E_z^{scat}}{\partial y^2} - k_0^2 \varepsilon_{rc} E_z^{scat} = k_0^2(\varepsilon_{rc}-1)E_z^{inc}. \quad (7)$$

The solution of (7) using the proposed method for this example is done as follows:

1. Initialize the values for w_{jx}, w_{jy}, v_j, and u_j using MATLAB function "rand" where $j = 1, 2, \ldots, 5$. The ANN was trained using a grid of 1000×1000 equidistant points in $\rho \in [0, \sqrt{50}]$ and $\emptyset \in [0, 2\pi]$, i.e., $h_x = 1000$, $h_y = 1000$, $c_x = 1, 2, 3, \ldots, h_x$ and $c_y = 1, 2, 3, \ldots, h_y$ in (4).

2. Determine the trial solution using (3). For 2D given examples, the problem is converted to cylindrical coordinate, and the trial solution in cylindrical coordinate for PEC case is

$$y_t(\emptyset,\rho,p) = E^{scat}_{ztrial}(\emptyset,\rho,p)$$

$$= A_1 \frac{(\rho-\rho_2)(\rho-\rho_3)\ldots(\rho-\rho_n)}{(\rho_1-\rho_2)(\rho_1-\rho_3)\ldots(\rho_1-\rho_n)} \times \frac{(\emptyset-\emptyset_2)(\emptyset-\emptyset_3)\ldots(\emptyset-\emptyset_n)}{(\emptyset_1-\emptyset_2)(\emptyset_1-\emptyset_3)\ldots(\emptyset_1-\emptyset_n)}$$

$$+ A_2 \frac{(\rho-\rho_1)(\rho-\rho_3)\ldots(\rho-\rho_n)}{(\rho_2-\rho_1)(\rho_2-\rho_3)\ldots(\rho_2-\rho_n)}$$

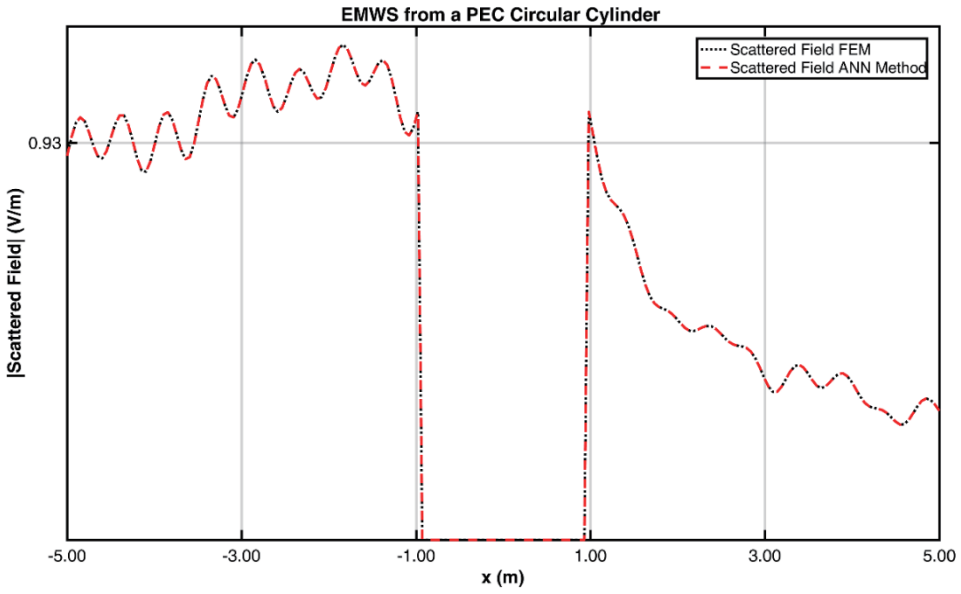

FIGURE 5. Absolute value for the scattered field solved by ANN method and FEM.

$$\times \frac{(\emptyset-\emptyset_1)(\emptyset-\emptyset_3)\ldots(\emptyset-\emptyset_n)}{(\emptyset_2-\emptyset_1)(\emptyset_2-\emptyset_3)\ldots(\emptyset_2-\emptyset_n)}$$

$$+\ldots+A_n\frac{(\rho-\rho_1)(\rho-\rho_2)\ldots(\rho-\rho_{n-1})}{(\rho_n-\rho_1)(\rho_n-\rho_2)\ldots(\rho_n-\rho_{n-1})}$$

$$\times \frac{(\emptyset-\emptyset_1)(\emptyset-\emptyset_2)\ldots(\emptyset-\emptyset_{n-1})}{(\emptyset_n-\emptyset_1)(\emptyset_n-\emptyset_2)\ldots(\emptyset_n-\emptyset_{n-1})}$$

$$+(\rho-\rho_1)(\emptyset-\emptyset_1)(\rho-\rho_2)(\emptyset-\emptyset_2)(\rho-\rho_3)$$
$$(\emptyset-\emptyset_3)\ldots(\rho-\rho_n)(\emptyset-\emptyset_n)\,N(\emptyset,\rho,p)$$

where ρ and $\emptyset$ are the standard cylindrical coordinate system [1]; A_1, A_2, ..., A_n are the BC values at the surface of the scatterer and found using $E_z^{scat}=-E_z^{inc}$, $(\rho_1,\emptyset_1)$; $(\rho_2,\emptyset_2)$, ..., $(\rho_n,\emptyset_n)$ are the locations of the BCs; n is the number of BC points,

$$N(\emptyset,\rho,p) = \frac{v_1}{1+e^{-(w_{1x}\rho\cos\emptyset+w_{1y}\rho\sin\emptyset+u_1)}} + \frac{v_2}{1+e^{-(w_{2x}\rho\cos\emptyset+w_{2y}\rho\sin\emptyset+u_2)}} + \frac{v_3}{1+e^{-(w_{3x}\rho\cos\emptyset+w_{3y}\rho\sin\emptyset+u_3)}} + \frac{v_4}{1+e^{-(w_{4x}\rho\cos\emptyset+w_{4y}\rho\sin\emptyset+u_4)}} + \frac{v_5}{1+e^{-(w_{5x}\rho\cos\emptyset+w_{5y}\rho\sin\emptyset+u_5)}}$$

where the coordinate transformation equations are used, i.e., $x=\rho\cos\emptyset$ and $y=\rho\sin\emptyset$ [1].

3. Use (4) to find the error, i.e.,

$$E(x,y,p) = \sum_{c_y=1}^{h_y}\sum_{c_x=1}^{h_x}\frac{1}{2}\left(\left(-\frac{\partial^2 y_t(x_{c_x},y_{c_y},p)}{\partial x^2}-\frac{\partial^2 y_t(x_{c_x},y_{c_y},p)}{\partial y^2}\right.\right.$$
$$\left.\left.-k_0^2\varepsilon_{rc}y_t\left(x_{c_x},y_{c_y},p\right)\right)-k_0^2(\varepsilon_{rc}-1)E_z^{inc}\right)^2.$$

4. Check the error, if the error $\leq$ the required error, stop. Otherwise, use (5) to adjust the old values of w_{jx}, w_{jy}, v_j, and u_j.

5. Repeat step 3 until you get the required error.

For dielectric case, the same discussed procedure is used except $A(\emptyset,\rho)=0$, and the trial solution is

$$y_t(\emptyset,\rho,p) = E_{ztrial}^{scat}(\emptyset,\rho,p) = N(\emptyset,\rho,p)$$

where the same training set for the previous example is used.

The proposed method is used to find E_{ztrial}^{scat} for a PEC and dielectric ($\varepsilon_r=4$) cylinder with radius $=\lambda$. The MSEs are 1.38×10^{-3} and 2.09×10^{-3} for a PEC and dielectric cylinder, respectively for all points of solution. The problem has been solved with $-5\leq x\leq 5$ m and $-5\leq y\leq 5$ m. Figs. 5 and 6 show the absolute of the scattered field at the middle of the problem, i.e., $-5\leq x\leq 5$ m and $y=0$ m.

3.3. Three Dimensional EMWS

The problem to be considered is EMWS from PEC or a dielectric sphere. Since the domain of interest extends to infinity, UPML is used. The incident field for this example is assumed to be $E_x^{inc}=\exp(-jk_0z)\hat{a}_x$ where $\hat{a}_x$ is the unit vector along the direction of incidence. Also, $f=3\times10^8/\lambda$ Hz and $\lambda=1$ m are assumed.

The solution of (1) using the proposed method for this example is done as follows:

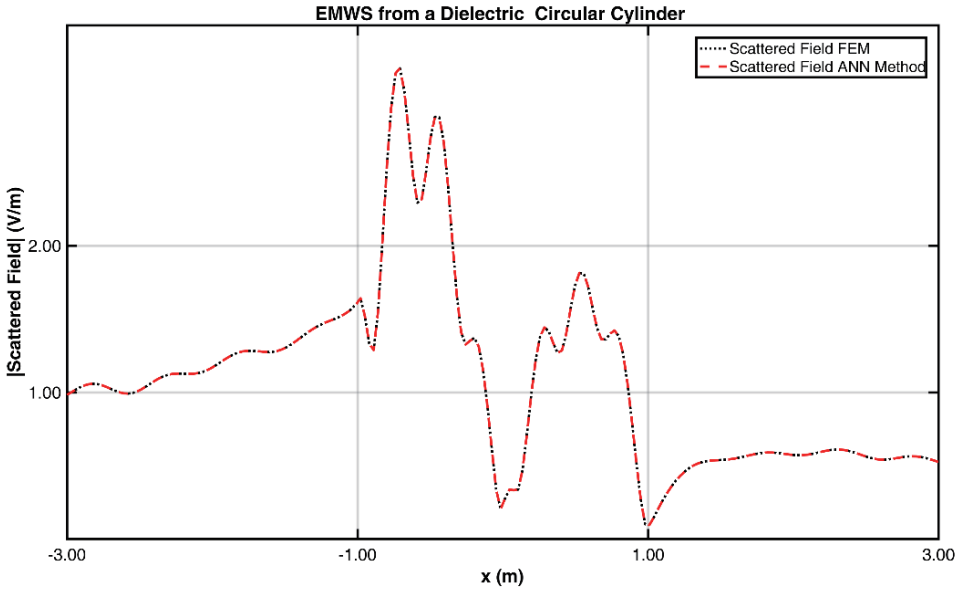

FIGURE 6. Absolute value for the scattered field solved by ANN method and FEM.

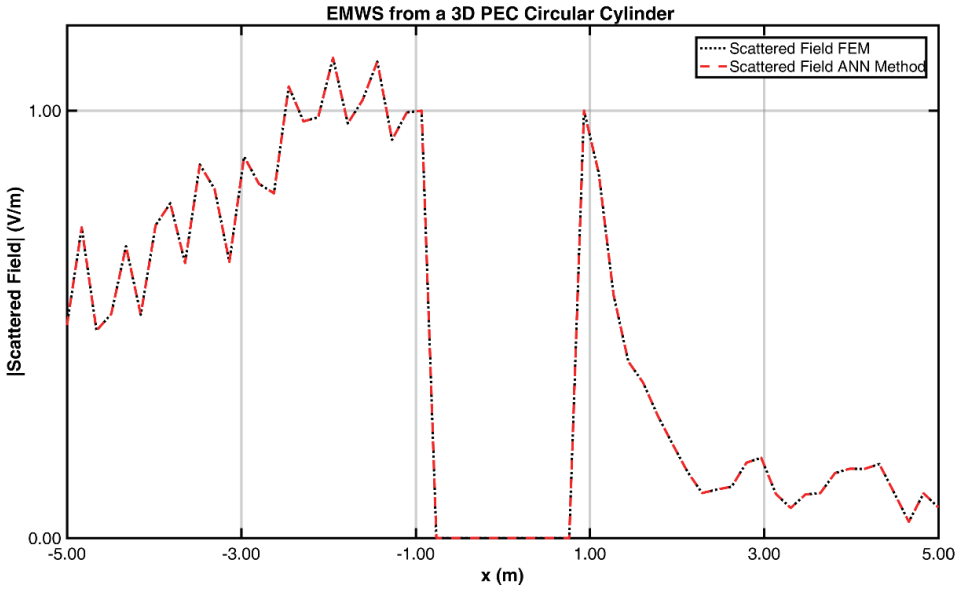

FIGURE 7. Absolute value for the scattered field solved by ANN method and FEM.

1. Initialize the values for w_{jx}, w_{jy}, w_{jz}, v_j, and u_j using MATLAB function "rand" where $j = 1, 2, \ldots, 5$. The ANN was trained using a grid of $1000 \times 1000 \times 1000$ equidistant points in $r \in [0, \sqrt{50}]$, $\theta \in [0, 2\pi]$ and $\emptyset \in [0, \pi]$, i.e., $h_x = 1000$, $h_y = 1000$, $h_z = 1000$, $c_x = 1, 2, 3, \ldots, h_x$, $c_y = 1, 2, 3, \ldots, h_y$ and $c_z = 1, 2, 3, \ldots, h_z$ in (4).

2. Determine the trial solution using (3). For PEC case, the problem is converted to spherical coordinate, and the trial solution in spherical coordinate is

$$y_t(r, \theta, \emptyset, p) = E^{scat}_{ztrial}(r, \theta, \emptyset, p)$$

$$= A_1 \frac{(r - r_2)(r - r_3) \ldots (r - r_n)}{(r_1 - r_2)(r_1 - r_3) \ldots (r_1 - r_n)} \times \frac{(\theta - \theta_2)(\theta - \theta_3) \ldots (\theta - \theta_n)}{(\theta_1 - \theta_2)(\theta_1 - \theta_3) \ldots (\theta_1 - \theta_n)} \times \frac{(\emptyset - \emptyset_2)(\emptyset - \emptyset_3) \ldots (\emptyset - \emptyset_n)}{(\emptyset_1 - \emptyset_2)(\emptyset_1 - \emptyset_3) \ldots (\emptyset_1 - \emptyset_n)} + A_2 \frac{(r - r_1)(r - r_3) \ldots (r - r_n)}{(r_2 - r_1)(r_2 - r_3) \ldots (r_2 - r_n)} \times \frac{(\theta - \theta_1)(\theta - \theta_3) \ldots (\theta - \theta_n)}{(\theta_2 - \theta_1)(\theta_2 - \theta_3) \ldots (\theta_2 - \theta_n)}$$

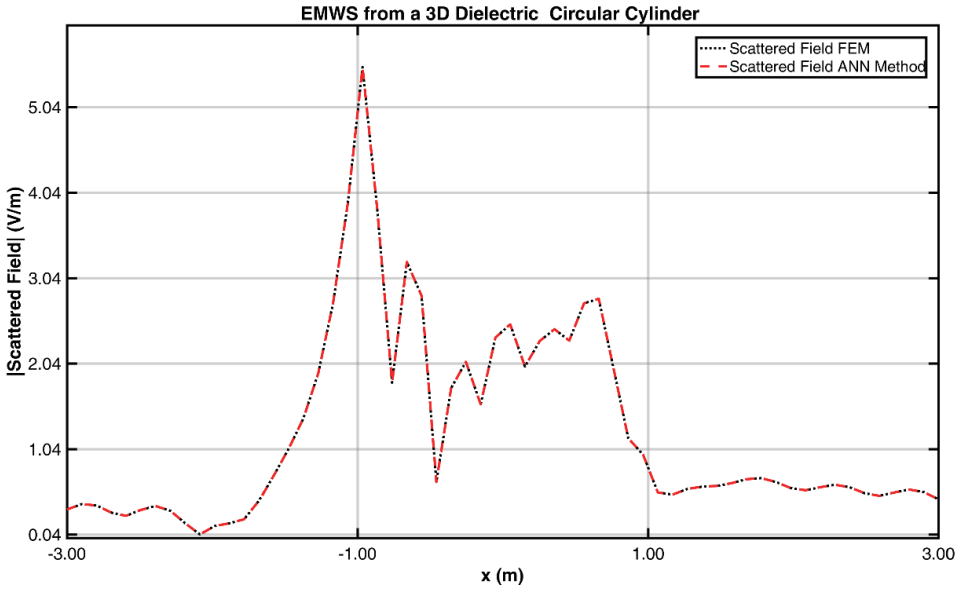

FIGURE 8. Absolute value for the scattered field solved by ANN method and FEM.

$$\times\frac{(\emptyset-\emptyset_1)(\emptyset-\emptyset_3)\ldots(\emptyset-\emptyset_n)}{(\emptyset_2-\emptyset_1)(\emptyset_2-\emptyset_3)\ldots(\emptyset_2-\emptyset_n)}+\ldots$$
$$+A_n\frac{(r-r_1)(r-r_2)\ldots(r-r_{n-1})}{(r_n-r_1)(r_n-r_2)\ldots(r_n-r_{n-1})}$$
$$\times\frac{(\theta-\theta_1)(\theta-\theta_2)\ldots(\theta-\theta_{n-1})}{(\theta_n-\theta_1)(\theta_n-\theta_2)\ldots(\theta_n-\theta_{n-1})}$$
$$\times\frac{(\emptyset-\emptyset_1)(\emptyset-\emptyset_2)\ldots(\emptyset-\emptyset_{n-1})}{(\emptyset_n-\emptyset_1)(\emptyset_n-\emptyset_2)\ldots(\emptyset_n-\emptyset_{n-1})}$$
$$+(r-r_1)(\theta-\theta_1)(\emptyset-\emptyset_1)(r-r_2)(\theta-\theta_2)$$
$$(\emptyset-\emptyset_2)\ldots(r-r_n)(\theta-\theta_n)(\emptyset-\emptyset_n)$$
$$N(r,\theta,\emptyset,p)$$

where r, θ, and $\emptyset$ are the standard spherical coordinate system [1]; A_1, A_2, ..., A_n are the BC values at the surface of the scatterer and can be found using $E_z^{scat}=-E_z^{inc}$; $(r_1,\theta_1,\emptyset_1)$, $(r_2,\theta_2,\emptyset_2)$, ..., $(r_n,\theta_n,\emptyset_n)$ are the locations of the BCs; n is the number of BC points, where

$$N(r,\theta,\emptyset,p)$$
$$=\frac{v_1}{1+e^{-(w_{1x}r\sin\theta\cos\emptyset+w_{1y}r\sin\theta\sin\emptyset+w_{1z}r\cos\theta+u_1)}}$$
$$+\frac{v_2}{1+e^{-(w_{2x}r\sin\theta\cos\emptyset+w_{2y}r\sin\theta\sin\emptyset+w_{2z}r\cos\theta+u_2)}}$$
$$+\frac{v_3}{1+e^{-(w_{3x}r\sin\theta\cos\emptyset+w_{3y}r\sin\theta\sin\emptyset+w_{3z}r\cos\theta+u_3)}}$$
$$+\frac{v_4}{1+e^{-(w_{4x}r\sin\theta\cos\emptyset+w_{4y}r\sin\theta\sin\emptyset+w_{4z}r\cos\theta+u_4)}}$$
$$+\frac{v_5}{1+e^{-(w_{5x}r\sin\theta\cos\emptyset+w_{5y}r\sin\theta\sin\emptyset+w_{5z}r\cos\theta+u_5)}}$$

where coordinate transformation is used, i.e., $x=r\sin\theta\cos\emptyset$, $y=r\sin\theta\sin\emptyset$, and $z=r\cos\theta$ [1].

3. Use (4) to find the error, i.e.,

$$E(x,y,z,p)=\sum_{c_z=1}^{h_z}\sum_{c_y=1}^{h_y}\sum_{c_x=1}^{h_x}$$
$$\frac{1}{2}\left(\left(-\frac{\partial^2 y_t(x_{c_x},y_{c_y},z_{c_z},p)}{\partial x^2}-\frac{\partial^2 y_t(x_{c_x},y_{c_y},z_{c_z},p)}{\partial y^2}\right.\right.$$
$$\left.-\frac{\partial^2 y_t(x_{c_x},y_{c_y},z_{c_z},p)}{\partial z^2}-k_0^2\varepsilon_{rc}y_t(x_{c_x},y_{c_y},z_{c_z},p)\right)$$
$$\left.-k_0^2(\varepsilon_{rc}-1)E_x^{inc}\right)^2.$$

4. Check the error, if the error $\leq$ the required error, stop. If not, use (5) to adjust the old values of w_{jx}, w_{jy}, w_{jz}, v_j, and u_j.

5. Repeat step 3 until you get the required error.

For dielectric case, the same procedure for the previous example is used, but the trial solution is

$$y_t(r,\theta,\emptyset,p)=E_{ztrial}^{scat}(r,\theta,\emptyset,p)=N(r,\theta,\emptyset,p).$$

The E_{ztrial}^{scat} for a PEC and dielectric ($\varepsilon_r=4$) sphere with radius $=\lambda$ at $z=0$ are solved using the proposed method, and the MSEs are 1.87×10^{-3} and 8.04×10^{-3} for a PEC and dielectric sphere, respectively for all points of the solution. The problem has been solved with $-5\leq x\leq 5$ m, $-5\leq y\leq 5$ m, and $-5\leq z\leq 5$ m. Figs. 7 and 8 show the absolute values of the scattered field at the middle of the problem, i.e., $-5\leq x\leq 5$ m, $y=0$ m, and $z=0$ m.

Figure 9 shows how the proposed method will go to the solution for selected number of epochs. As the dimension of the problem increases, the number of epochs will increase to get the required accuracy.

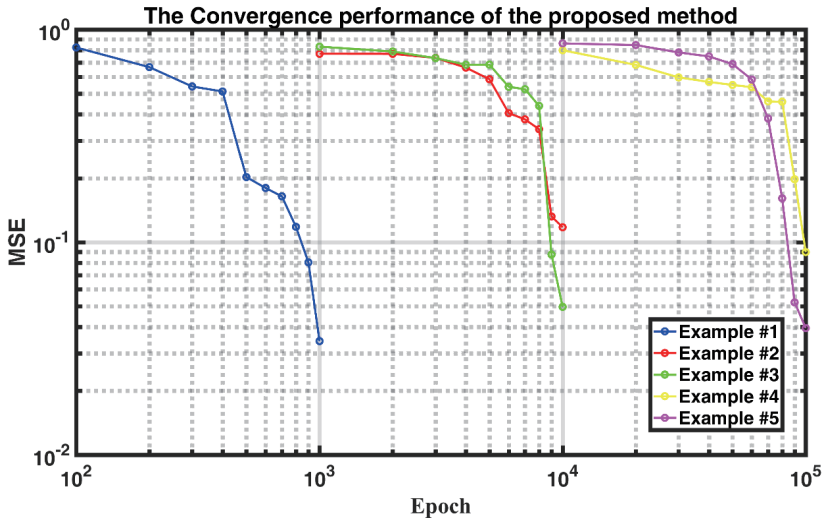

FIGURE 9. The MSE versus epoch for the given examples.

TABLE 1. Time Comparison between FEM and ANN required to solve previous examples.

Dimension	Example	FEM (sec)	ANN (sec)
1D	A lossy dielectric slab	1.0091	112.65
2D	PEC	4.2739	342.77
	Dielectric	6.5728	563.26
3D	PEC	16.8390	1154.97
	Dielectric	26.1392	1791.72

Table 1 summarizes the time required to solve the examples in the proposed method versus FEM.

It is clear that FEM is faster than the proposed method. Also, the proposed ANN is a basic form of ANNs. It is expected, as a future research, by using more advanced ANNs, that the time required to solve the problem will be reduced. In addition, building the matrices that are required to use FEM is difficult and becomes more difficult in 3D cases in contrast with the proposed method.

4. CONCLUSION

An approach using ANN has been proposed to solve 2-ODE that represents EMWS. Its implementation is simple and straightforward in comparison with the traditional methods, i.e., MoM, FEM, and FDM, and the results are accurate. Also, the approach is general and only requires creating a correct form of the trial solution. Future work should include studying the effect of using more than one hidden layer in the ANNs on the efficiency of the method and the effect of choosing the learning parameter on the speed of convergence to the solution.

REFERENCES

[1] Warnick, K. F., *Numerical Methods For Engineering An Introduction Using Matlab and Computational Electromagnetics Examples*, 2nd ed., The Institution of Engineering and Technology, Croydon, UK, 2020.

[2] Jin, J., *The Finite Element Method in Electromagnetics*, 3rd ed., Wiley, IEEE Press, NY, USA, 2014.

[3] Özgün, O. and M. Kuzuoğlu, *Matlab-based Finite Element Programming in Electromagnetic Modeling*, 1st ed., CRC Press, Taylor & Francis Group, FL, USA, 2019.

[4] Taflove, A. and S. C. Hagness, *Computational Electrodynamics: The Finite-difference Time-domain Method*, 3rd ed., Artech House, MA, USA, 2005.

[5] Elsherbeni, A. and V. Demir, *The Finite-Difference Time-Domain Method for Electromagnetics with MATLAB Simulations*, 2nd ed., SciTech Publishing Inc., NJ, USA, 2016.

[6] Harrington, R. F., *Field Computation by Moment Methods*, Wiley-IEEE Press, NY, USA, 1993.

[7] Gibson, W. C., *The Method of Moments in Electromagnetics*, 3rd ed., CRC Press, NY, USA, 2021.

[8] Olshanskii, M. A. and E. E. Tyrtyshnikov, *Iterative Methods For Linear Systems: Theory and Applications*, SIAM, PHL, USA, 2014.

[9] Glassner, A., *Deep Learning: A Visual Approach*, No Starch Press, CA, USA, 2021.

[10] Krizhevsky, A., I. Sutskever, and G. E. Hinton, "Imagenet classification with deep convolutional neural networks," *Proc. 25th Int. Conf. Neural Inf. Process. Syst.*, 1097–1105, 2013.

[11] Ibtehaz, N. and M. S. Rahman, "MultiResUNet: Rethinking the U-Net architecture for multimodal biomedical image segmentation," *Neural Networks*, Vol. 121, 74–87, Jan. 2020.

[12] Fahad, S. K. A. and A. E. Yahya, "Inflectional review of deep learning on natural language processing," in *2018 International Conference on Smart Computing and Electronic Enterprise (ICSCEE)*, Shah Alam, Malaysia, Jul. 2018.

[13] Wang, Y., "Cognitive foundations of knowledge science and deep knowledge learning by cognitive robots," in *2017 IEEE 16th International Conference on Cognitive Informatics & Cognitive Computing (ICCI)*, 5, 2017.

[14] Jafar-Zanjani, S., M. M. Salary, D. Huynh, E. Elhamifar, and H. Mosallaei, "Tco-based active dielectric metasurfaces design by conditional generative adversarial networks," *Advanced Theory and Simulations*, Vol. 4, No. 2, Feb. 2021.

[15] Bae, M., J. Jo, M. Lee, J. Kang, S. V. Boriskina, and H. Chung, "Inverse design and optical vortex manipulation for thin-film absorption enhancement," *Nanophotonics*, Vol. 12, No. 22, 4239–4254, 2023.

[16] Kudyshev, Z. A., D. Sychev, Z. Martin, O. Yesilyurt, S. I. Bogdanov, X. Xu, P.-G. Chen, A. V. Kildishev, A. Boltasseva, and V. M. Shalaev, "Machine learning assisted quantum super-resolution microscopy," *Nature Communications*, Vol. 14, No. 1, Aug. 2023.

[17] Qi, S., Y. Wang, Y. Li, X. Wu, Q. Ren, and Y. Ren, "Two-dimensional electromagnetic solver based on deep learning technique," *IEEE Journal on Multiscale and Multiphysics Computational Techniques*, Vol. 5, 83–88, 2020.

[18] Guo, R., Z. Lin, T. Shan, M. Li, F. Yang, S. Xu, and A. Abubakar, "Solving combined field integral equation with deep neural network for 2-D conducting object," *IEEE Antennas and Wireless Propagation Letters*, Vol. 20, No. 4, 538–542, Apr. 2021.

[19] Massa, A., D. Marcantonio, X. Chen, M. Li, and M. Salucci, "Dnns as applied to electromagnetics, antennas, and propagationa review," *IEEE Antennas and Wireless Propagation Letters*, Vol. 18, No. 11, 2225–2229, Nov. 2019.

[20] Alzahed, A. M., S. M. Mikki, and Y. M. M. Antar, "Nonlinear mutual coupling compensation operator design using a novel electromagnetic machine learning paradigm," *IEEE Antennas and Wireless Propagation Letters*, Vol. 18, No. 5, 861–865, May 2019.

[21] Giannakis, I., A. Giannopoulos, and C. Warren, "A machine learning-based fast-forward solver for ground penetrating radar with application to full-waveform inversion," *IEEE Transactions on Geoscience and Remote Sensing*, Vol. 57, No. 7, 4417–4426, Jul. 2019.

[22] Chen, S., H. Wang, F. Xu, and Y.-Q. Jin, "Target classification using the deep convolutional networks for SAR images," *IEEE Transactions on Geoscience and Remote Sensing*, Vol. 54, No. 8, 4806–4817, Aug. 2016.

[23] Lagaris, I. E., A. Likas, and D. I. Fotiadis, "Artificial neural networks for solving ordinary and partial differential equations," *IEEE Transactions on Neural Networks*, Vol. 9, No. 5, 987–1000, Sep. 1998.

[24] Lagaris, I. E., A. C. Likas, and D. G. Papageorgiou, "Neural-network methods for boundary value problems with irregular boundaries," *IEEE Transactions on Neural Networks*, Vol. 11, No. 5, 1041–1049, Sep. 2000.

[25] McFall, K. S. and J. R. Mahan, "Artificial neural network method for solution of boundary value problems with exact satisfaction of arbitrary boundary conditions," *IEEE Transactions on Neural Networks*, Vol. 20, No. 8, 1221–1233, Aug. 2009.

[26] Anitescu, C., E. Atroshchenko, N. Alajlan, and T. Rabczuk, "Artificial neural network methods for the solution of second order boundary value problems," *Cmc-computers Materials & Continua*, Vol. 59, No. 1, 345–359, 2019.

[27] Abdolrazzaghi, M., S. Hashemy, and A. Abdolali, "Fast-forward solver for inhomogeneous media using machine learning methods: artificial neural network, support vector machine and fuzzy logic," *Neural Computing & Applications*, Vol. 29, No. 12, 1583–1591, Jun. 2018.

[28] Nitta, T., "An extension of the back-propagation algorithm to complex numbers," *Neural Networks*, Vol. 10, No. 8, 1391–1415, Nov. 1997.